Deformation and Fracture Behavior of Polypropylene–Ethylene Vinyl Alcohol Blends Compatibilized with Ionomer Zn^{2+}

M. Montoya,[1] M. J. Abad,[1] L. Barral Losada,[1] C. Bernal[2]

[1]*Grupo de Polímeros, Departamento de Física, E.U.P.-Ferrol, Universidad de A Coruña, Avda. 19 Febrero, s/n. 15405-Ferrol, Spain*
[2]*Instituto de Investigaciones en Ciencia y Tecnología de Materiales, Universidad Nacional de Mar del Plata, Argentina, Juan B. Justo 4302, B7608FDQ Mar del Plata, Argentina*

Received 18 August 2004; accepted 18 January 2005
DOI 10.1002/app.22175
Published online in Wiley InterScience (www.interscience.wiley.com).

ABSTRACT: This work investigated the deformation and fracture behavior of polypropylene–ethylene vinyl alcohol (PP/EVOH) blends compatibilized with ionomer Zn^{2+}. Uniaxial tensile tests and quasistatic fracture experiments were performed for neat PP and for 10 and 20 wt % EVOH blends with different ionomer contents. The addition of EVOH copolymer to PP led to an increase in the Young's modulus whereas the yield strength was decreased with the EVOH content as a consequence of the higher stiffness of EVOH and the poor interfacial adhesion between PP and EVOH, respectively. Furthermore, the incorporation of EVOH into PP promoted stable crack growth. Neat PP displayed nonlinear load-displacement behavior with some amount of slow crack growth preceding unstable brittle fracture, whereas most PP/EVOH blends exhibited "pseudostable" fracture characterized by slow crack growth that could not be externally controlled. All blends exhibited lower resistance to crack initiation than PP but the fracture propagation resistance was significantly improved. For 10 wt % EVOH blends, the resistance to crack initiation was roughly constant with the ionomer content up to 5%, then it increased with the further addition of compatibilizer. Conversely, for 20 wt % EVOH blends, the resistance to crack initiation appeared to be independent of the ionomer content. The better resistance to crack initiation exhibited by the 10 wt % EVOH blends could be attributed to a higher level of compatibilization in these blends. By contrast, 20 wt % EVOH blends with $\leq$2% ionomer content showed completely stable crack growth. In addition, *J–R* curves and valid plane strain fracture toughness values for these blends could also be determined. © 2005 Wiley Periodicals, Inc. J Appl Polym Sci 98: 1271–1279, 2005

Key words: polypropylene blends; mechanical properties; fracture

INTRODUCTION

Obtaining a low-cost material for packaging and hydrocarbons transport is still a difficult problem to solve because simultaneous barrier and mechanical properties are required. Ease of processing at low cost, recyclability, and optical clarity (especially for food packaging) are also needed. A common practice in industry is to blend a small quantity of a barrier material into a low-cost material to obtain a low-cost product with improved barrier properties.[1]

Polypropylene (PP) is a useful commodity polymer with good mechanical and barrier properties to water that can be used for food packaging. However, its applications are limited because of its poor barrier properties to oxygen. In contrast, the copolymer of ethylene and vinyl alcohol (EVOH) has high barrier properties to oxygen and carbon dioxide,[1,2] as well as high resistance to hydrocarbons and good processability.[3] Hence, the combination of both polymers offers an alternative to produce a low-cost material with good barrier properties.[1]

For materials to be used in structural or semistructural applications, adequate fracture properties are also required. Commercial PP homopolymer usually has the disadvantage of being quite brittle at room temperature and exhibiting poor resistance to crack propagation.[4] Several studies regarding the tensile properties of PP/EVOH blends have been published,[1,3,5,6] and significant efforts have been devoted to the fracture behavior of impact-modified PP blends.[7–12] However, at the time of writing no toughness data or fracture behavior studies have been reported for PP/EVOH blends, thus limiting the use of these blends as structural materials.

This work investigated the deformation and fracture behavior of PP/EVOH blends compatibilized with ionomer Zn^{2+}. Uniaxial tensile tests on dumbbell-shaped samples and fracture tests on single-edge

Correspondence to: C. Bernal (crbernal@fi.mdp.edu.ar).
Contract grant sponsor: CONICET.

TABLE I
Melting Points Determined by DSC

	T_{m1} (°C)	T_{m2} (°C)
PP	159.1	—
PP/EVOH/ionomer Zn^{2+} blends (%)		
90/10	160.3	182.5
90/10/2	161.8	182.3
90/10/5	158.7	182.5
90/10/10	159.8	182.5
80/20	161.3	182.3
80/20/2	160.4	182.9
80/20/5	161.0	183.5
80/20/10	158.4	182.9
EVOH	—	181.8

The heating rate was 10°C/min with a precision of ±1°C.

notched bending (SENB) specimens were performed for neat PP and for 10 and 20 wt % EVOH blends with different ionomer content.

EXPERIMENTAL

Materials

An extrusion grade of PP was synthesized by Repsol (ISPLEN PP044W3f). Its melt flow index (MFI) value is 3.02 g/10 min (230°C, 2160 g) and density is 0.90 g cm^{-3}. The EVOH copolymer (F101B grade, EVAL Europe) has an ethylene content of 32.9%, an MFI of 1.51 g/10 min (190°C, 2160 g), and density of 1.19 g cm^{-3}. Because PP and EVOH have poor miscibility,[5] ionomer Zn^{2+} was used as a compatibilizer.

The ionomer Zn^{2+} (Surlyn 9970, Du Pont) is a random ethylene/methacrylic acid copolymer with an MFI of 14 g/10 min (190°C, 2160 g) and density of 0.94 g cm^{-3}. It was expected that the ionomer Zn^{2+} would interact by complexation with the OH groups of EVOH.[3]

The melting points of the pure components and the blends determined by differential scanning calorimetry are listed in Table I.

Blend preparation

Prior to processing, EVOH and ionomer Zn^{2+} were dried in a vacuum oven for 24 h at 80°C and 8 h at 60°C, respectively. Blends of PP/EVOH and PP/EVOH/ionomer Zn^{2+} were prepared using a corotating twin-screw extruder (Brabender DSE20) operating at a speed of 45 rpm. The barrel temperature was 215°C and the die temperature was 220°C. All components were premixed by tumbling and simultaneously fed into the twin-screw extruder.

Binary blends were prepared in 90/10 and 80/20 (w/w) PP/EVOH proportions. The compatibilized blends were made with 2, 5, and 10% of ionomer Zn^{2+} with respect to the EVOH mass in the blend.

Sample preparation and mechanical characterization

Pellets of the blends were compression molded into plaques at 220°C under 1-MPa pressure for 15 min followed by 10 MPa for 8 min. Then, the plaques were rapidly cooled by circulating water within the press plates under a pressure of 10 MPa. The thermal stresses generated during molding were released by annealing the plaques in an oven for 3 h at 100°C.

Uniaxial tensile tests were carried out on type IV ASTM D638-93 dumbbell-shaped specimens cut from compression-molded plates of 3-mm thickness in a tensile testing dynamometer (model 4467) at 5 mm/min. The tensile modulus and yield strength were determined from the true stress–strain curves. Short and long travel incremental mechanical extensometers were used for obtaining the Young's modulus and the whole stress–strain curve, respectively.

Fracture characterization was carried out on SENB specimens cut from compression-molded thick plaques [thickness (B) = 8 mm].

Sharp notches were introduced by sliding a fresh razor blade into a machined slot. Crack/depth (a/W), thickness/depth (B/W), and span/depth (S/W) ratios were maintained at 0.5, 0.5, and 4, respectively.

Fracture tests were performed in three-point bending in the tensile testing dynamometer with a crosshead speed of 1 mm/min. These tests consisted of loading the specimens to subcritical displacement levels and then unloading. Complete fracture of specimens was attained at high velocity in a Charpy pendulum after they had been immersed in liquid nitrogen for a few minutes. Crack extension (Δa) was determined from the fracture surface using an optical microscope.

The resistance to crack initiation was characterized by the critical stress intensity factor (K_{IQ}), calculated from the maximum in the load-displacement curves[13]:

$$K_{IQ} = f(a/W)P_{max}/(BW^{1/2}) \quad (1)$$

where P_{max} is the maximum load and $f(a/W)$ is a function of the a/W ratio. If linear elastic fracture mechanics is applicable, K_{IQ} can be taken as the plane strain critical stress intensity factor (K_{IC}).[12]

For those blends that exhibited completely stable crack propagation behavior, J-integral crack growth resistance (J vs. Δa) curves were also determined by the normalization method as explained elsewhere[14–16] and by the multiple specimen technique in accordance with the ESIS protocol recommendations.[17] All mechanical tests were carried out at room temperature.

Scanning electron microscopy (SEM) fractography

The fracture surfaces of SENB specimens were examined using a Jeol JSM-6400 SEM microscope at an

accelerating voltage of 20 kV. The samples were sputter coated with a thin layer of gold before they were observed.

RESULTS AND DISCUSSION

Morphological analysis

The fracture surface for neat PP revealed that some amount of stable crack growth followed by unstable brittle fracture existed in this material [Fig. 1(a)]. For the blends, regardless of the compatibilizer content [Fig. 1(b,c)], matrix ductile tearing could be distinguished from the unstable fracture, which was promoted by the high velocity and low temperature in the Charpy pendulum. Otherwise, ductile tearing (slow crack growth) would have been extended through the whole ligament because it was verified by testing several samples for each composition until complete fracture.

Figures 2 and 3 show SEM microphotographs of the fast cryofractured surface region for the PP/EVOH blends with 10 and 20 wt % EVOH, respectively. The blend morphology is composed of the PP matrix containing spheres of EVOH. It is clearly seen in Figure 2(a) and Figure 3(a,b) that the dispersed phase underwent debonding on fracture and no rests of the PP matrix are observed, suggesting poor interfacial adhesion between both phases.[5] In contrast, the increase in the ionomer Zn^{2+} content led to more homogeneous blends and the second-phase particle size decreased, confirming the compatibilizing effect of ionomer Zn^{2+}. For the 10 wt % EVOH blend, even for an ionomer content as low as 2%, the particles were almost indistinguishable [Fig. 2(b)].

In addition, EVOH particles were found to be smaller for the 10 wt % EVOH blends [compare Figs. 2(a) and 3(a)], as expected.

Closer views of the stable crack propagation zone for samples of 10 wt % EVOH blends (Fig. 4) also show the matrix ductile tearing among second-phase EVOH particles, and these particles became less distinguishable as the ionomer content increased.

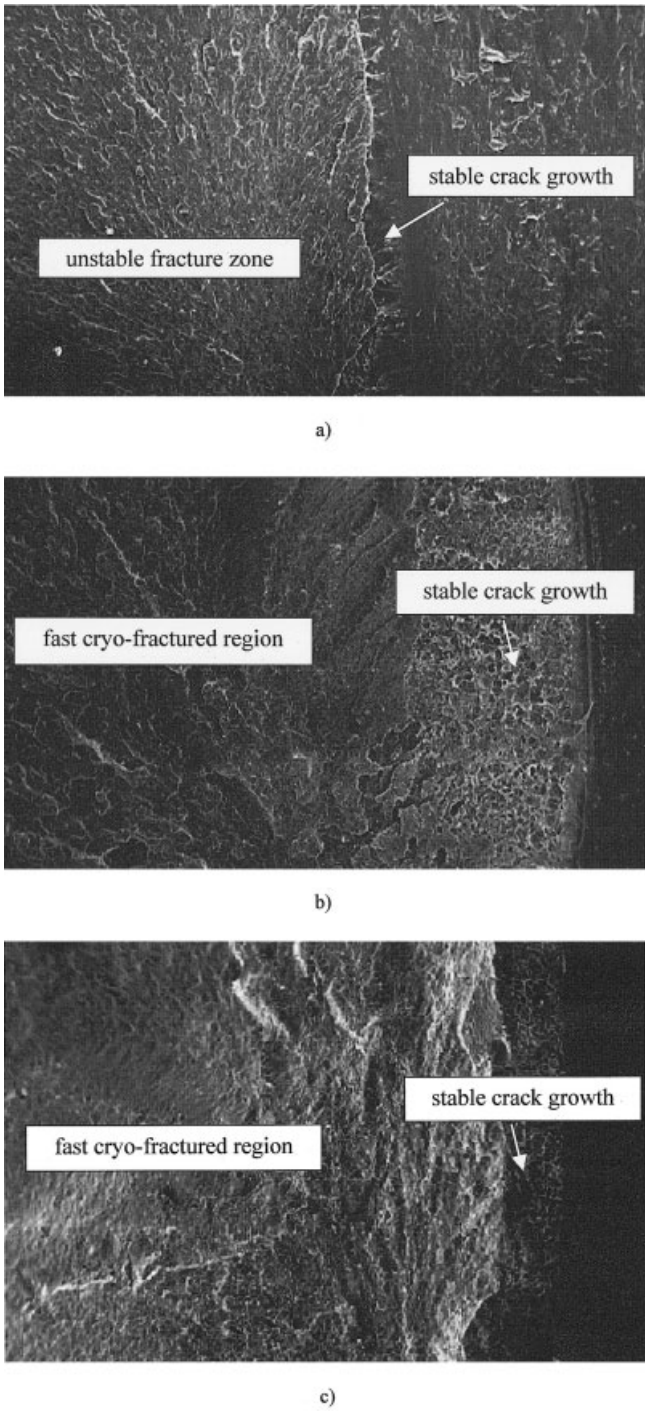

Figure 1 SEM micrographs of the fracture surface of single-edge notched bending samples at an original magnification ×20 (crack propagated from the right to the left): (a) neat PP, (b) 10 wt % EVOH blend, and (c) 20 wt % EVOH blend.

Deformation behavior

Figure 5(a,b) shows typical true stress–strain curves for pure PP and for the blends with 10 and 20 wt % of EVOH at different ionomer Zn^{2+} content, respectively. All PP samples displayed ductile behavior that was characterized by a decrease in stress after yield (strain softening) followed by a steep rise of stress until failure occurred. However, most of the PP/EVOH samples did not exhibit strain hardening. All blends displayed less ductility than pure PP as a result of the poor interfacial adhesion between both phases and the subsequent particle debonding. Young's modulus and yield strength were determined from these curves. The results are presented in Figure 6.

As can be observed in Figure 6(a), the Young's modulus increases with the EVOH content according to expectations because the elastic modulus of EVOH is considerably higher than that of PP.[1] In contrast, a

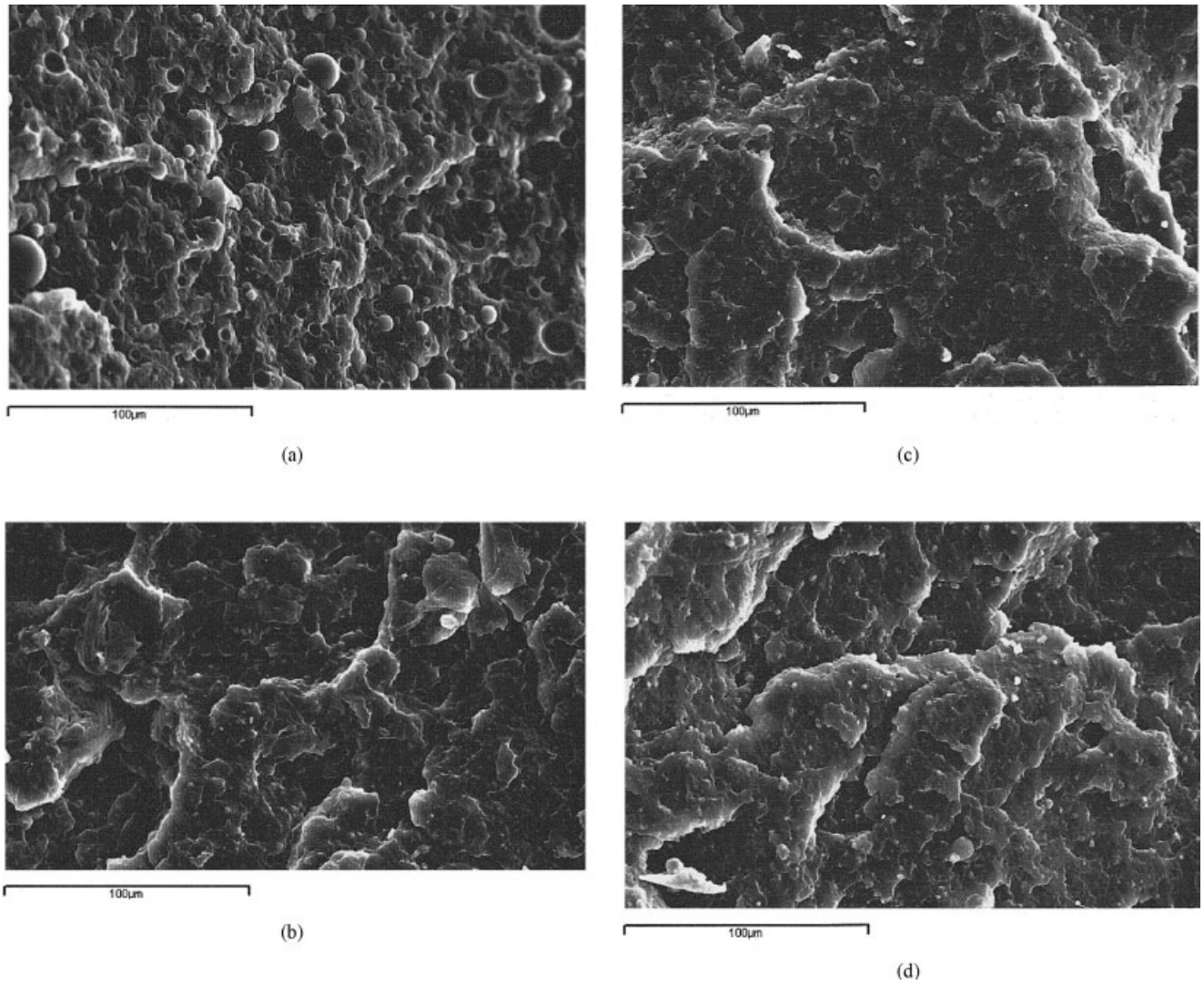

Figure 2 SEM microphotographs of the fast cryofractured surface region for 10 wt % EVOH blends at ionomer Zn^{2+} contents of (a) 0, (b) 2, (c) 5, and (d) 10%; scale bar = 100 μm.

decreasing trend of the Young's modulus with ionomer content was observed, which was due to the low modulus of the ionomer Zn^{2+}.[18] However, regardless of the ionomer content, all blends still exhibited higher stiffness than pure PP.

In contrast, there was a decreasing trend of yield strength with EVOH content [Fig. 6(b)], in agreement with other findings, which was probably attributable to debonding between PP and EVOH.[1] Wong and Mai[11] established that poor tensile strength and low failure strain were caused by particle debonding from the matrix prior to yielding as a result of poor interfacial adhesion. However, no significant differences in yield strength with the ionomer Zn^{2+} content for each EVOH composition were found.

It is also interesting to note that macroscopic observation of uniaxial samples after failure indicated that PP samples developed a well-defined stress-whitened neck that stabilized and fractured with many shear bands. Conversely, in the PP/EVOH blend specimens, the neck was unable to stabilize and continued to thin down until failure.

Fracture behavior

Figure 7 shows the normalized load as P/B^2 versus displacement traces for SENB specimens of neat PP and the blends with 10 and 20 wt % EVOH.

Neat PP exhibited nonlinear load-displacement behavior with some amount of slow crack growth preceding unstable fracture, which agrees with the results reported in the literature for PP homopolymer.[4,19] In the initial steps, stable crack propagation was observed. At a certain point in the load-displacement curve, the propagation mode suddenly changed. Crack propagation became unstable and the samples separated into two halves.[19] Then, the *J*-integral pa-

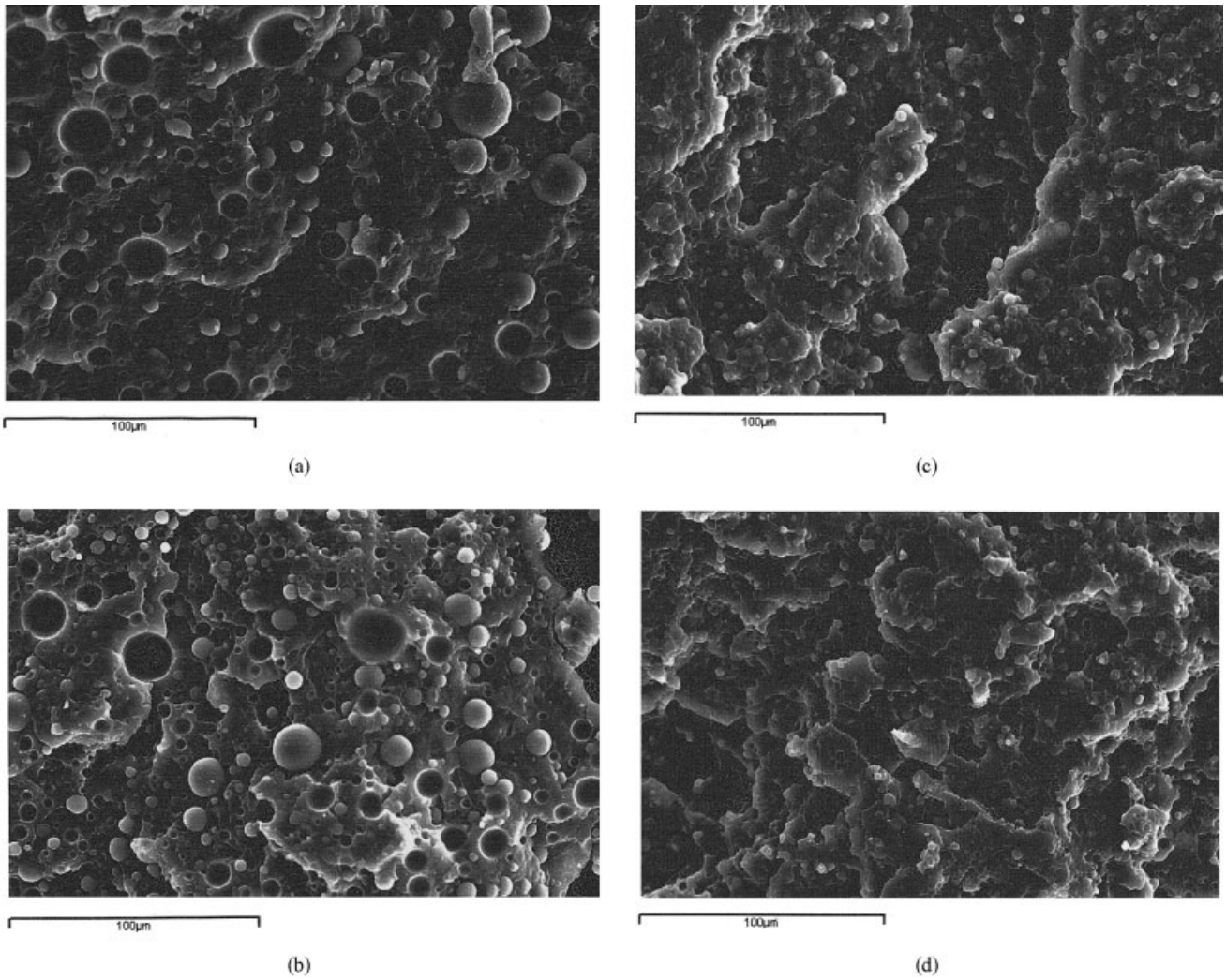

Figure 3 SEM microphotographs of the fast cryofractured surface region for 20 wt % EVOH blends at ionomer Zn^{2+} contents of (a) 0, (b) 2, (c) 5, and (d) 10%; scale bar = 100 μm.

rameter at instability (*Jc*), which can be used for quasibrittle fracture characterization,[20] was adopted for this material. The *Jc* value was found to be 10.2 ± 0.4 kJ/m^2, which is within the range of values reported in the literature for PP homopolymer under static loading conditions.[4,19] Furthermore, it was previously reported that the toughness of different PP homopolymers can vary widely.[21]

In contrast, all PP/EVOH blends displayed nonlinear load-displacement behavior with apparently stable crack growth (Fig. 7) and without any evidence of sudden instability. In addition, fracture surfaces and side views of broken specimens were stress whitened. However, except for 20 wt % EVOH blends with ionomer Zn^{2+} content lower than 2%, crack extension could not be externally controlled and the crack continued growing, even after the test had been interrupted. This behavior is referred to here as "pseudostable" behavior.

In the light of the different behaviors displayed by the materials, any parameter able to give comparative values of fracture resistance had to be used.

According to linear elastic fracture mechanics,[22] for valid plane strain fracture toughness determinations, the linear-elastic behavior up to the point of fracture and plane strain conditions are simultaneously required. Although these requirements were not satisfied in our experiments, the K_{IQ} values still reflect a critical stress state for crack initiation.[12] Hence, they were used here to compare the fracture initiation behavior of all blends, and the results are shown in Figure 8. All PP/EVOH blends displayed lower values of resistance to crack initiation than pure PP, probably due to the presence of critical-size flaws derived from debonding of second-phase particles that induced premature failure.[11]

For the 10 wt % EVOH blend, the K_{IQ} value was found to be roughly constant up to 5% ionomer Zn^{2+};

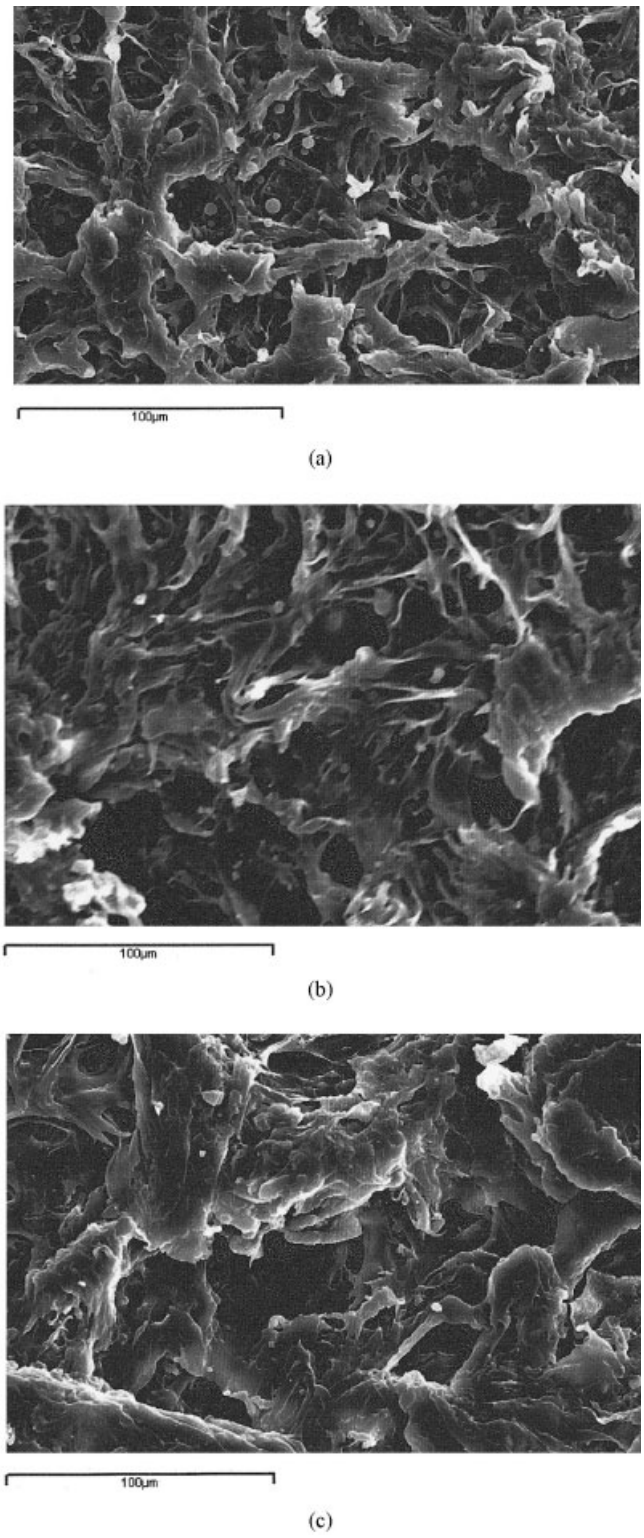

Figure 4 Closer views of the slow crack growth zone of (a) 90/10/2, (b) 90/10/5, and (c) 90/10/10 blends; scale bar = 100 μm.

then, it was slightly increased with further addition of compatibilizer. In contrast, this parameter was not markedly affected by the compatibilizer content for 20 wt % EVOH blends. This difference in the trend of the resistance to crack initiation can be explained in terms of the different morphologies displayed by the blends. As explained earlier, the incorporation of ionomer Zn^{2+} promoted the formation of more homogeneous blends as well as a decrease in the second-phase particle size. This effect was more pronounced for 10 wt % EVOH blends. The formation of critical-size flaws able to induce premature failure is likely to be suppressed as the particle size decreases.[11] Therefore, the better fracture resistance to crack initiation displayed by 10 wt % EVOH blends for ionomer Zn^{2+} content higher than 5% can be attributed to a decrease in the critical-size flaw formation in smaller EVOH particles.

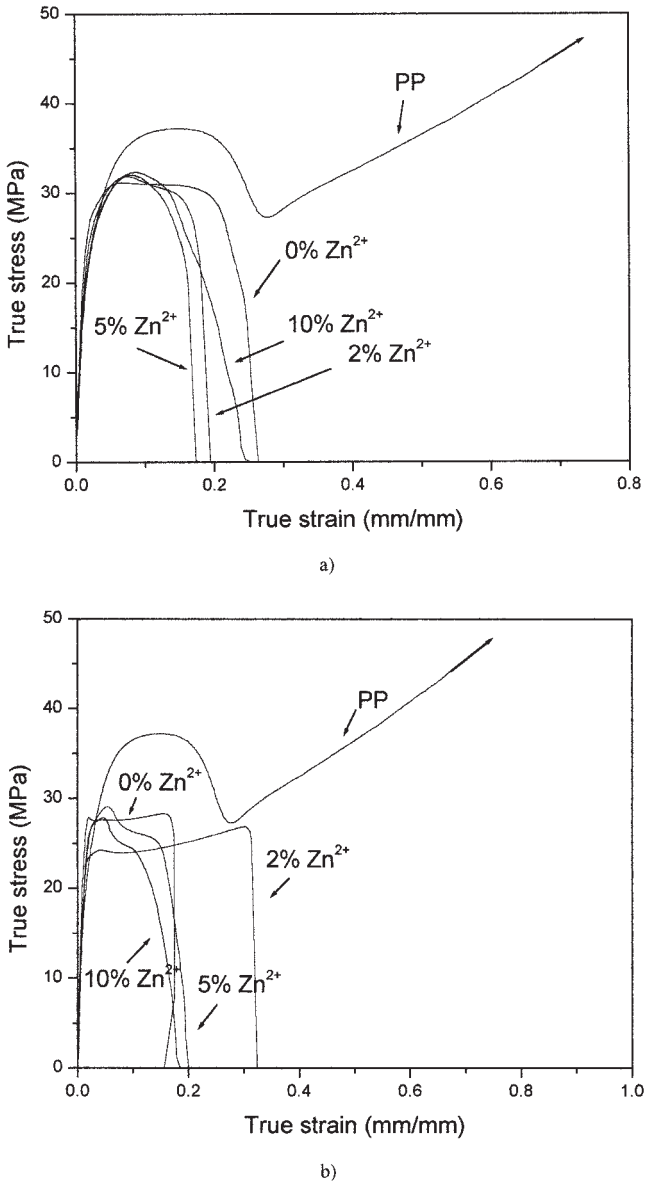

Figure 5 True stress–strain curves for pure polypropylene and the blends with different ionomer Zn^{2+} content: (a) 10 wt % EVOH blends and (b) 20 wt % EVOH blends.

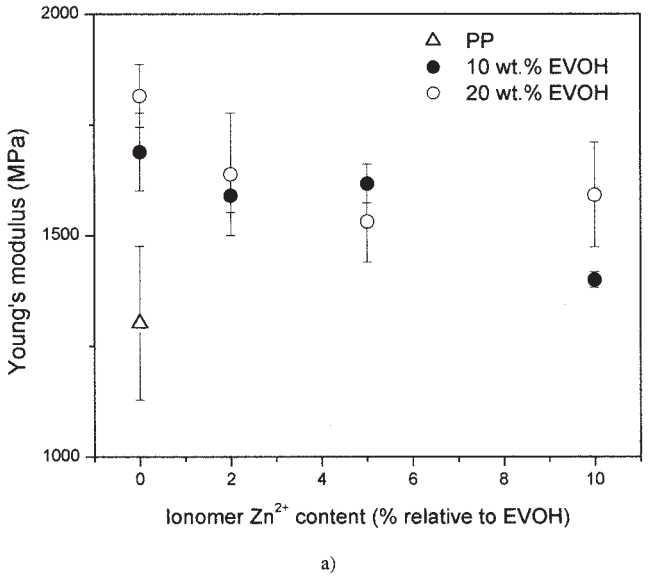

Figure 6 The tensile properties as a function of ionomer Zn^{2+} content for 10 and 20 wt % EVOH blends: (a) Young's modulus and (b) yield strength.

Although the incorporation of EVOH into PP was detrimental to the resistance to crack initiation, a significant improvement in the crack propagation resistance was found as more energy was absorbed by the blend specimens to fracture, which is represented by the area under the load-displacement curve in Figure 7. Poor adhesion between PP and EVOH was responsible for debonding at the PP/EVOH interface and hence for inducing matrix stretching and work hardening, which required a large amount of energy. Debonding at the interface also prevented the unstable fracture due to void coalescence that occurs in pure PP.[23,24]

In contrast, samples of 20 wt % EVOH blends having ionomer content of ≤2% displayed completely

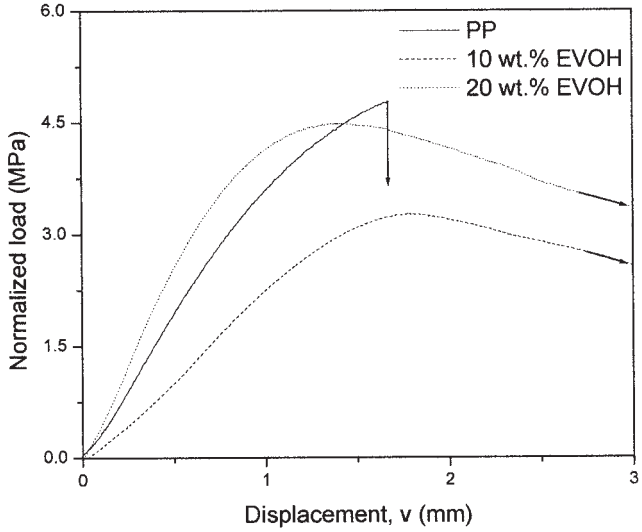

Figure 7 Normalized load-displacement traces for neat PP and the 10 and 20 wt % EVOH blends.

stable crack growth with higher levels of lateral stress whitening. For these blends, *J–R* curves were obtained by the normalization method[14–16] as well as by the multiple specimen technique as a reference[15] [Fig. 9(a,b)]. Furthermore, different records were analyzed in order to further check the validity of the *J–R* curves obtained by the normalization method, as suggested by Morhain and Velasco.[25] These curves for different samples (Fig. 9) are superimposed in a single curve, which also fall within the experimental scatter of multiple specimen data points, suggesting that valid *J–R* curves were obtained. The critical initiation parameter (J_{IC}) was determined from these curves, in accordance with the European protocol recommendations[17] from

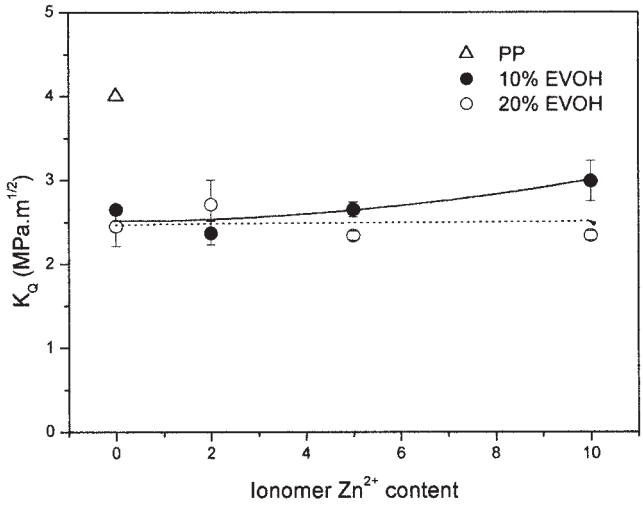

Figure 8 The critical stress intensity factor (K_{IQ}) as a function of ionomer Zn^{2+} content for 10 and 20 wt % EVOH blends.

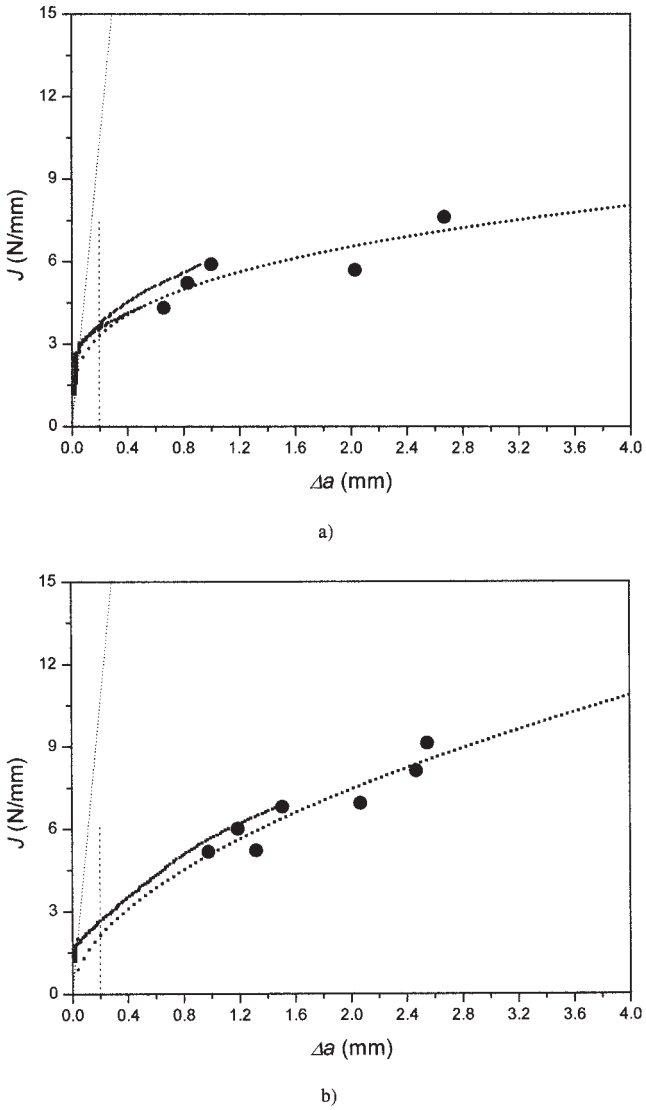

Figure 9 *J*-Integral versus crack extension (Δa) curves for the blends that displayed completely stable crack growth: (a) 80/20/0 blend and (b) 80/20/2 blend.

the intersection of a vertical line at 0.2-mm crack growth with the best fit of the J–Δa data. The values obtained are reported in Table II, along with the minimum thickness requirement for the plane strain condition,[17] which was always met for the sample thickness used in this work (B = 8 mm). Hence, the J_{IC} values determined here represented valid plane strain fracture toughness values.

As also observed from Table II, the same trend for the K_{IQ} parameter with EVOH and ionomer Zn^{2+} content was found for K_{ICJ} obtained from J_{IC} values as:

$$K_{ICJ} = J_{IC}E/(1 - v^2) \quad (2)$$

with Poisson's ratio (ν) taken as 0.4.[26]

The results obtained here are similar to those reported by Vu-Khahn and Fisa for filled PP.[23,24] In their works, the fillers were found to enhance a more widespread crack growth at the microscopic level; hence, more stable failure by fracture was observed. Microscopic damage induced by debonding at the matrix/filler interface was assumed to be responsible for this behavior.[23] They also observed opposite trends in crack initiation and crack propagation resistances with filler size. The fracture resistance at initiation increased as the filler size decreased whereas the energy absorbed by the fracture process decreased and the material became less resistant to unstable fracture. The resistance to crack growth of mica-reinforced PP was found to depend on the competition between voiding and matrix stretching.[24]

In our PP/EVOH blends, more stable fracture was also observed that was due to the presence of second-phase EVOH particles in the PP matrix. In addition, the completely stable fracture behavior displayed by 20 wt % EVOH blends with ionomer content lower than 2%, which also have larger EVOH particles, was attributed to the combined effect of particle size and poor adhesion between PP and EVOH.

CONCLUSIONS

The deformation and fracture behavior of PP/EVOH blends compatibilized with ionomer Zn^{2+} was investigated. Morphological analysis of PP/EVOH blends confirmed the compatibilizing effect of the ionomer Zn^{2+} because more homogeneous blends were obtained and the second-phase particle size decreased with ionomer content. The 10 wt % EVOH blends exhibited smaller second-phase particles.

The addition of EVOH copolymer to PP led to an increase in the Young's modulus whereas the yield strength was decreased with the EVOH content as a consequence of the higher stiffness of EVOH and the debonding of particles from the matrix, respectively.

All PP/EVOH blends exhibited lower values of resistance to crack initiation in comparison to the neat PP, which was probably due to the presence of critical-size flaws derived from debonding of second-phase particles.[11]

The 10 wt % EVOH blends showed better fracture resistance to crack initiation. This result can be attrib-

TABLE II
Fracture Initiation Parameter Values

	J_{IC} (kJ/m^2)	B_{min} (mm)	K_{ICJ} (MPa m$^{1/2}$)
PP	10.2 ± 0.4	7.5	4.0
PP/EVOH/ionomer Zn^{2+} blends (%)			
80/20/0	3.8 ± 0.2	3.5	2.9
80/20/2	3.0 ± 0.4	2.9	2.4

uted to the decrease of critical-size flaw formation as a consequence of the presence of smaller EVOH particles in these blends.

The incorporation of EVOH into PP promotes stable crack growth, as reflected in the fracture experiments. Neat PP displayed nonlinear load-displacement behavior with some amount of slow crack growth preceding unstable brittle fracture. In contrast, most of the PP/EVOH blends exhibited pseudostable fracture that was characterized by uncontrollable slow crack growth. Therefore, the resistance to crack propagation was significantly improved as more energy was absorbed by the blend specimens to fracture as a consequence of the matrix plastic deformation induced by debonding at the EVOH–PP interface.

In addition, 20 wt % EVOH blends with ionomer content $\leq$2% showed completely stable crack growth and therefore *J–R* curves could be determined for these blends. Valid plane strain fracture toughness values were obtained accordingly.

The authors thank CONICET for financial support.

References

1. Faisant, J. B.; Ait-Kadi, A.; Bousmina, M.; Deschenes, L. Polymer 1998, 39, 533.
2. Demarquette, N. R.; Kamal, M. R. J Appl Polym Sci 1998, 70, 75.
3. Kalfoglou, N. K.; Samios, C. K.; Papadopoulou, C. P. J Appl Polym Sci 1998, 68, 589.
4. Frontini, P. M.; Fave, A. J Mater Sci 1995, 30, 2446.
5. Abad, M. J.; Ares, A.; Barral, L.; Cano, J.; Díez, F. J.; García-Garabal, S.; López, J.; Ramírez, C. J Appl Polym Sci, to appear.
6. Abad, M. J.; Ares, A.; Barral, L.; Eguiazábal, J. I. Polym Int, to appear.
7. van del Wal, A.; Nijhol, R.; Gaymans, R. J. Polymer 1999, 40, 6031.
8. van del Wal, A.; Gaymans, R. J. Polymer 1999, 40, 6045.
9. van del Wal, A.; Verheul, A. J. J.; Gaymans, R. J. Polymer 1999, 40, 6057.
10. van del Wal, A.; Gaymans, R. J. Polymer 1999, 40, 6067.
11. Wong, S.-C.; Mai, Y.-W. Polymer 1999, 40, 1553.
12. Gensler, R.; Plummer, C. J. G.; Grein, C.; Kausch, H. H. Polymer 2000, 41, 3809.
13. Williams, J. G. In Fracture Mechanics of Polymers; Ellis Horwood Limited: London, 1984.
14. Bernal, C. R.; Cassanelli, A. N.; Frontini, P. M. Polym Test 1995, 14, 85.
15. Bernal, C. R.; Montemartini, P. E.; Frontini, P. M. J Polym Sci Part B: Polym Phys 1996, 34, 1869.
16. Bernal, C.; Rink, M.; Frontini, P. Macromol Symp 1999, 147, 235.
17. A Testing Protocol for Conducting *J*-Crack Growth Resistance Curve Tests on Plastics. ESIS-TC4 Polymers and Composites; Hale, G.E., Ed.; Cambridge University Press: Cambridge, UK, 1991.
18. Kim, Y.; Ha, C.-S.; Kang, T.-K.; Kim, Y.; Cho, W.-J. J Appl Polym Sci 1994, 51, 1453.
19. Santarelli, E.; Frontini, P. Polym Eng Sci 2001, 41, 1803.
20. Fasce, L.; Frontini, P. J Macromol Sci Phys 2002, B41, 1231.
21. Hodgkinson, J. M.; Savadori, A.; Williams, J. G. J Mater Sci 1983, 18, 2319.
22. Standard Test Methods for Plane-Strain Fracture Toughness and Energy Release Rate Determination of Plastics Materials; ASTM D5045–93; American Society for Testing and Materials: New York, 1993.
23. Vu-Khanh, T.; Fisa, B. Theor Appl Fracture Mech 1990, 13, 11.
24. Vu-Khanh, T.; Fisa, B. Polym Compos 1986, 77, 219.
25. Morhain, C.; Velasco, I. J Mater Sci 2001, 36, 1487.
26. Fasce, L. Ph.D. Thesis, Mar del Plata, 2002.